

# Tunable single-photon multi-channel quantum router based on a hybrid optomechanical system

Peng-Cheng Ma<sup>1,2,3</sup>, Jian-Qi Zhang<sup>2,\*</sup>, Yin Xiao<sup>1</sup>, Mang Feng<sup>2,†</sup> and Zhi-Ming Zhang<sup>1‡</sup>

<sup>1</sup>*Laboratory of Nanophotonic Functional Materials and Devices (SIPSE),  
and Laboratory of Quantum Engineering and Quantum Materials,  
South China Normal University, Guangzhou 510006, China*

<sup>2</sup>*State Key Laboratory of Magnetic Resonance and Atomic and Molecular Physics,  
Wuhan Institute of Physics and Mathematics, Chinese Academy of Sciences, Wuhan 430071, China*

<sup>3</sup>*School of Physics and Electronic Electrical Engineering,  
Huaiyin Normal University, Huaian 223300, China*

Routing of photon play a key role in optical communication networks and quantum networks. Although the quantum routing of signals has been investigated in various systems both in theory and experiment, the general form of quantum routing with multi-output terminals still needs to be explored. Here, we propose an experimentally accessible tunable single-photon multi-channel routing scheme using a optomechanics cavity coulomb coupling to a nanomechanical resonator. The router can extract a single-photon from the coherent input signal directly modulate into three different output channels. More important, the two output signal frequencies can be selected by adjusting Coulomb coupling strength. We also demonstrate the vacuum and thermal noise will be insignificant for the optical performance of the single-photon router at temperature of the order of 20 mK. Our proposal may have paved a new avenue towards multi-channel router and quantum network.

PACS numbers: 42.50.Ex, 03.67.Hk, 41.20.Cv

Quantum information science has been developed rapidly due to the substitution of photons as signal carriers rather than the limited electrons [1]. Single photons are suitable candidates as the carrier of quantum information due to the fact that they propagate fast and interact rarely with the environment. Meanwhile, a quantum single-photons router is challenging because the interaction between individual photons is generally very weak. Quantum router or quantum switch plays a key role in optical communication networks and quantum information processing. It is important for controlling the path of the quantum signal with fixed Internet Protocol (IP) addresses, or quantum switch without fixed IP addresses.

Designing a quantum router or an optical switch operated at a single photon level enables a selective quantum channel in quantum information and quantum networks [2–9], such as in different systems of quantum router, cavity QED system [10], circuit QED system [3], optomechanical system [4], a pure linear optical system [11, 12],  $\Lambda$ -type three-level system [13–15]. The essence lying at the core is the realization of the strong coupling between the photons and photons or photons and phonons [17–20], but these methods require high-pump-laser powers due to the very weak optical nonlinearity. To the best of our knowledge, the quantum router demonstrated in most experiments and theoretical proposals has only one output terminal, except for only a few theoretical method in Ref. [13–16] and the experiments in Ref.[12]. However,

the two output ports are composited the two photonic crystal cavities [13] or two coupled-resonator waveguides [14, 15] whose two output channels with a maximal probability of unity and no more than 1/2, respectively. And the Ref.[16] is the extended to N output ports from the method [14]. Thus the ideal quantum router with multi-channel deserves based on only one cavity with an extremely high probability still need to be explored. In the following, we propose a new scheme, via Coulomb coupling interaction, one can realize one input signal with three output signals based on only one optical cavity mode with unity probability. Our proposal is essentially different from previous methods in Ref.[13–15] that we are able to directly modulate the coherent input signal into three different output ports.

In this letter, we theoretical propose a scheme for single-photon quantum routing with three output ports based on a optomechanics cavity Coulomb coupling to a nanomechanical resonator (NMR). More important, the two output signals frequencies can be selected by adjusting Coulomb coupling strength. The thermal noise could be more critical in deteriorating the performance of the single-photon router. Then, we also demonstrate the vacuum and thermal noise can be insignificant for the optical performance of the single-photon router at temperature of the order of 20 mK.

*Model setup and the solutions.*— The model for realizing single-photon routing is sketched in Fig. 1, where a partially transparent nanomechanical mirror (NMM) which is charged with the bias voltage  $V_1$  placed at the middle position of Fabry-Perot cavity formed by two fixed mirrors that have finite identical transmission [21]. The whole cavity length is  $L$ . The cavity field is driven by a

\*Electronic address: boing777@qq.com

†Electronic address: mangfeng@wipm.ac.cn

‡Electronic address: zmzhang@scnu.edu.cn

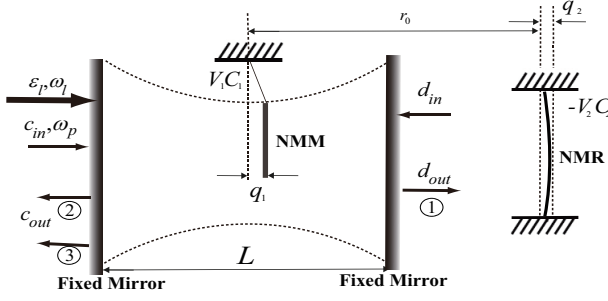


FIG. 1: Schematic diagram of the system. A high-quality Fabry-Perot cavity consists of two fixed mirrors and a NMM. NMM is charged by the bias gate voltage  $V_1$  and subject to the Coulomb force due to the charged NMR with the bias gate voltage  $V_2$ . The optomechanical cavity of the length  $L$  is driven by two light fields, one of which is the pump field  $\varepsilon_l$  with the frequency  $\omega_l$  and the other of which is the probe field  $c_{in}$  with the frequency  $\omega_p$ . The output field is represented by  $c_{out}$  and  $d_{out}$ .  $q_1$  and  $q_2$  represent the small displacements of the NMM and NMR from their equilibrium positions, with  $r_0$  is the equilibrium distance between them.

strong coupling field at frequency  $\omega_l$  from the left-hand mirror. Further, the field in a single-photon Fock state at frequency  $\omega_p$  is incident on the cavity through the left-hand mirror. Besides the radiation pressure force coupling the NMM to the cavity mode, the NMM is also subject to Coulomb force to the charged NMR with the bias gate voltage  $-V_2$  near by the cavity.  $q_1$  and  $q_2$  represent the small displacements of the NMM and the NMR around their equilibrium positions,  $r_0$  is the distance between their equilibrium position. Then the Hamiltonian of the whole system can be written as

$$H_{whole} = \hbar\omega_c c^\dagger c + \sum_{j=1}^2 \left( \frac{p_j^2}{2m_j} + \frac{1}{2} m_j \omega_j^2 q_j^2 \right) - \hbar g c^\dagger c q_1 + H_I + i\hbar \varepsilon_l (c^\dagger e^{-i\omega_l t} - H.C.), \quad (1)$$

where the first term is for the single-mode cavity field with frequency  $\omega_c$  and annihilation (creation) operator  $c$  ( $c^\dagger$ ). The second term describes the vibration of the charged NMM (NMR) with frequency  $\omega_1$  ( $\omega_2$ ) and effective mass  $m_1$  ( $m_2$ ),  $p_1$  ( $p_2$ ) and  $q_1$  ( $q_2$ ) are the momentum and the position operator of NMM (NMR), respectively [4]. The third term describe the radiation pressure coupling the cavity field to the NMM, with  $g = \frac{\omega_c}{L}$  is the coupling strength [21]. The last terms describe the interaction between the cavity field with the input fields. The pump field strength  $\varepsilon_l$ , depends on the power  $\wp$  of coupling field,  $\varepsilon_l = \sqrt{2\kappa\wp/\omega_l}$  with  $\kappa$  is the cavity decay rate.

The forth term  $H_I$  in Eq.(1) presents the Coulomb coupling between the charged NMM and NMR [22], where the NMM and NMR take the charges  $C_1 V_1$  and  $-C_2 V_2$ , with  $C_1$  and  $C_2$  are the capacitance of the gates, respectively. The interaction energy between the NMM and NMR is given by  $H_I = \frac{-C_1 V_1 C_2 V_2}{4\pi\epsilon_0 |r_0 + q_1 - q_2|}$ . In the case of

$q_1, q_2 \ll r_0$ , with the second order expansion, the above Hamiltonian is rewritten as  $H_I = \frac{-C_1 V_1 C_2 V_2}{4\pi\epsilon_0 r_0} [1 - \frac{q_1 - q_2}{r_0} + (\frac{q_1 - q_2}{r_0})^2]$ , where the linear term may be absorbed into the definition of the equilibrium positions, and the quadratic term includes a renormalization of the oscillation frequency for both the NMM and NMR. It implies a reduced form  $H_I = \hbar\lambda q_1 q_2$ , where  $\lambda = \frac{C_1 V_1 C_2 V_2}{2\pi\hbar\epsilon_0 r_0^3}$  [22].

In a frame rotating with the frequency  $\omega_l$  of the pump field, the Hamiltonian of the total system Eq.(1) can be rewritten as,

$$H_{total} = \hbar\Delta_c c^\dagger c + \sum_{j=1}^2 \left( \frac{p_j^2}{2m_j} + \frac{1}{2} m_j \omega_j^2 q_j^2 \right) - \hbar g c^\dagger c q_1 + \hbar\lambda q_1 q_2 + i\hbar \varepsilon_l (c^\dagger - c), \quad (2)$$

where  $\Delta_c = \omega_c - \omega_l$ . Note that the NMM and the NR coupled to the thermal surrounding at the temperature  $T$ , which results in the mechanical damping rate  $\gamma_1$  and  $\gamma_2$ , and thermal noise force  $\xi_1$  and  $\xi_2$  with frequency-domain correlation [4],

$$\langle \xi_\tau(\omega) \xi_\tau(\Omega) \rangle = 2\pi\hbar\gamma_\tau m_\tau \omega [1 + \coth(\frac{\hbar\omega}{2\kappa_B T})] \delta(\omega + \Omega), \quad (3)$$

where  $\tau=1$  or  $2$  and  $\kappa_B$  is the Boltzmann constant. In addition, the cavity field  $c$  is coupled to the input quantum fields  $c_{in}$  and  $d_{in}$ . If there are no photons incident from the right, then  $d_{in}$  would be the vacuum field. Let  $2\kappa$  be the rate at which photons leak out from each of the cavity mirrors. The output fields can be written as

$$x_{out}(\omega) = \sqrt{2\kappa} c(\omega) - x_{in}(\omega), \quad x = c, d. \quad (4)$$

These couplings are included in the standard way by writing quantum Langevin equations for the cavity field operators. Putting together all the quantum fields, thermal fluctuations, and the Heisenberg equations from the Hamiltonian (2), we can obtain the working quantum Langevin equations:

$$\begin{aligned} \dot{q}_1 &= \frac{p_1}{m_1}, \quad \dot{q}_2 = \frac{p_2}{m_2}, \\ \dot{c} &= -[2\kappa + i(\Delta_c - gq_1)]c + \varepsilon_l + \sqrt{2\kappa}c_{in} + \sqrt{2\kappa}d_{in}, \\ \dot{p}_1 &= -m_1\omega_1^2 q_1 - \hbar\lambda q_2 + \hbar g c^\dagger c - \gamma_1 p_1 + \xi_1, \\ \dot{p}_2 &= -m_2\omega_2^2 q_2 - \hbar\lambda q_1 - \gamma_2 p_2 + \xi_2, \end{aligned} \quad (5)$$

The quantum Langevin equations (5) can be solved after all operator are linearized as its steady-state mean value and a small fluctuation:

$$q_\tau = q_{\tau s} + \delta q_\tau, \quad p_\tau = p_{\tau s} + \delta p_\tau, \quad c = c_s + \delta c, \quad (6)$$

where  $\delta q_\tau$ ,  $\delta p_\tau$ ,  $\delta c$  being the small fluctuations around the corresponding steady values and  $\tau=1, 2$ . After substituting Eq.(6) into Eq.(5), ignoring the second-order small terms, and introducing the Fourier transforms  $f(t) = \frac{1}{2\pi} \int_{-\infty}^{+\infty} f(\omega) e^{-i\omega t} d\omega$ ,  $f^+(t) = \frac{1}{2\pi} \int_{-\infty}^{+\infty} f^*(-\omega) e^{-i\omega t} d\omega$ .

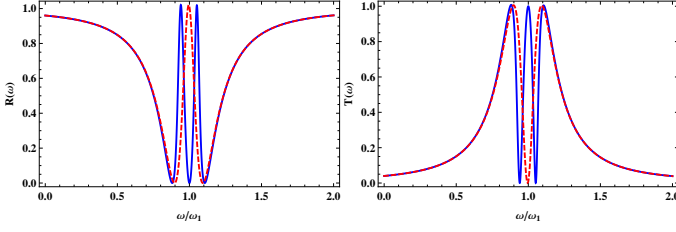


FIG. 2: (Color online) (a) The reflection spectrum  $R(\omega)$  and (b) the transmission spectrum  $T(\omega)$  of the single photon as a function of normalized frequency  $\omega/\omega_1$  when the Coulomb interaction is turned off (red dashed line) or turned on (blue solid line).  $\lambda_l = 1054$  nm,  $L = 6.7$  cm,  $\omega_1 = \omega_2 = 2\pi \times 134 \times 10^3$  Hz,  $Q_1 = Q_2 = 1.1 \times 10^6$ ,  $m_1 = m_2 = 40$  ng,  $\kappa = \omega_1/10$ ,  $\wp_l = 2$   $\mu$ W, and  $\lambda = 3 \times 10^{33}$  Hz/m<sup>2</sup>.

We can get the steady values

$$\begin{aligned} p_{1s} = p_{2s} = 0, \quad q_{1s} &= \frac{\hbar g |c_s|^2}{m_1 \omega_1^2 - \frac{\hbar^2 \lambda^2}{m_2 \omega_2^2}}, \\ q_{2s} &= \frac{\hbar \lambda q_{1s}}{-m_2 \omega_2^2}, \quad c_s = \frac{\varepsilon_l}{2\kappa + i\Delta}, \end{aligned} \quad (7)$$

with  $\Delta = \Delta_c - gq_{1s}$ , and the solution of  $\delta c$  [23],

$$\begin{aligned} \delta c &= E(\omega)c_{in}(\omega) + F(\omega)c_{in}^+(-\omega) + E(\omega)d_{in}(\omega) \\ &+ F(\omega)d_{in}^+(-\omega) + V_1(\omega)\xi_1(\omega) + V_2(\omega)\xi_2(\omega), \end{aligned} \quad (8)$$

in which

$$\begin{aligned} E(\omega) &= \sqrt{2\kappa} \left[ \frac{1}{2\kappa + i(\Delta - \omega)} \right. \\ &\quad \left. + \frac{ig^2 \hbar |c_s|^2 (2\kappa i + \Delta + \omega) m_2 (\omega^2 + i\omega\gamma_2 - \omega_2^2)}{d(\omega)} \right], \\ F(\omega) &= \frac{i\sqrt{2\kappa} g^2 \hbar |c_s|^2 (2\kappa i - \Delta + \omega) m_2 (\omega^2 + i\omega\gamma_2 - \omega_2^2)}{d(\omega)}, \\ V_1(\omega) &= \frac{g |c_s|^2 [(2\kappa i + \omega)^2 - \Delta^2] m_2 (\omega^2 + i\omega\gamma_2 - \omega_2^2)}{d(\omega)}, \\ V_2(\omega) &= \frac{g \hbar \lambda |c_s|^2 [(2\kappa i + \omega)^2 - \Delta^2]}{d(\omega)}, \end{aligned} \quad (9)$$

with

$$\begin{aligned} d(\omega) &= (2\kappa i + \Delta - \omega) \{ -\hbar^2 \lambda^2 [\Delta^2 + (2\kappa i + \omega)^2] \\ &+ m_2 (\omega^2 + i\omega\gamma_2 - \omega_2^2) [2 |c_s|^2 g^2 \hbar \Delta + (\Delta - 2\kappa i - \omega) \\ &\times (\Delta + 2\kappa i + \omega) m_1 (\omega^2 + i\omega\gamma_1 - \omega_1^2)] \}. \end{aligned} \quad (10)$$

Defining the spectrum of the field via  $\langle c^+(-\Omega)c(\omega) \rangle = 2\pi S_c(\omega)\delta(\omega + \Omega)$ ,  $\langle c(\omega)c^+(-\Omega) \rangle = 2\pi[S_c(\omega) + 1]\delta(\omega + \Omega)$ . The incoming vacuum field  $d_{in}$  is characterized by  $\langle d(\omega)d^+(-\Omega) \rangle = 2\pi\delta(\omega + \Omega)$  with  $S_{din}(\omega) = 0$ . From Eq. (4) and Eq. (8), we can obtain the spectrum of the output fields,

$$\begin{aligned} S_{cout}(\omega) &= R(\omega)S_{cin} + S^{(v)}(\omega) + S_1^T(\omega) + S_2^T(\omega), \\ S_{dout}(\omega) &= T(\omega)S_{cin} + S^{(v)}(\omega) + S_1^T(\omega) + S_2^T(\omega), \end{aligned} \quad (11)$$

where

$$\begin{aligned} R(\omega) &= |\sqrt{2\kappa}E(\omega) - 1|^2, \quad T(\omega) = |\sqrt{2\kappa}E(\omega)|^2, \\ S_1^T(\omega) &= 2\kappa |V_1(\omega)|^2 \hbar \gamma_1 m_1(-\omega) [1 + \coth(\frac{-\hbar\omega}{2\kappa_B T})], \\ S_2^T(\omega) &= 2\kappa |V_2(\omega)|^2 \hbar \gamma_2 m_2(-\omega) [1 + \coth(\frac{-\hbar\omega}{2\kappa_B T})], \\ S^{(v)}(\omega) &= 4\kappa |F(\omega)|^2. \end{aligned} \quad (12)$$

When there is no Coulomb coupling  $\lambda$  (*i.e.*  $\lambda = 0$ ) between the NMM and the NMR, Eq.(11) can be reduced to Eq.(10) in Ref.[4]. However, different from the output field in Ref.[4] involving a single output channel for quantum router, there are three output channels with different frequencies in our scheme due to Coulomb interaction. Further more, the frequencies of two output channel can be selected by adjusting the Coulomb coupling strength  $\lambda$ .

*Quantum routing for single photons.* — In Eq.(11),  $R(\omega)$  and  $T(\omega)$  are the contributions arising from the presence of a single photon in the input field.  $S^{(v)}(\omega)$  is the contribution from incoming vacuum field. The  $S_1^T(\omega)$  and  $S_2^T(\omega)$  are contributions from the fluctuation of the NMM and the NMR, respectively. Eq.(11) shows that even if there were no incoming photon, the output signal is generated via quantum and thermal noises. For the purpose of achieving a single-photon router, the key quantities are  $R(\omega)$  and  $T(\omega)$ . Further, we also demonstrate the performance of the single-photon router should not be deteriorated by the quantum and thermal noises terms  $S^{(v)}(\omega)$  and  $S_\tau^T(\omega)$  ( $\tau = 1, 2$ ).

To demonstrate the routing functions of our hybrid optomechanics system, we first investigate the reflection  $R(\omega)$  and transmission spectrum  $T(\omega)$ . For illustration of the numerical results, we choose the realistically reasonable parameters from the recent experiment [21] on the observation of the strong dispersive coupling between a cavity and the NMM. The wavelength of the pump field  $\lambda_l = 1054$  nm,  $L = 6.7$  cm,  $m_1 = m_2 = 40$  ng,  $\omega_1 = \omega_2 = 2\pi \times 134 \times 10^3$  Hz, quality factor  $Q_1 = Q_2 = 1.1 \times 10^6$ ,  $\gamma_1 = \gamma_2 = \frac{\omega_1}{Q_1} = 0.76$  s<sup>-1</sup>,  $\kappa = \frac{\omega_1}{10}$ ,  $\wp_l = 5$   $\mu$ W, we choose coulomb coupling strength  $\lambda = 3 \times 10^{33}$  Hz/m<sup>2</sup>. We also apply the following conditions [24, 25], (i)  $\Delta \simeq \omega_1$  and (ii)  $\omega_1 \gg \kappa$ . The first condition means that the optical cavity is driven by a red-detuned laser field which is on resonance with the optomechanical anti-Stokes sideband. The second condition is the well-known resolved sideband condition, which ensures the normal mode splitting to be distinguished [25].

The resulting spectra are shown in Figs 2 and 3. In the absence of the Coulomb coupling strength (*i.e.*  $\lambda = 0$ ), one observes an inverted EIT and a standard EIT in the reflection and transmission spectra of a single photon. Note the  $R(\omega_1) \approx 1$  and  $T(\omega) \approx 0$ . So the single photon is complete reflected through the cavity to the left output port. However, in the presence of the Coulomb coupling strength, the situation is completely different  $R(\omega_1) \approx 0$  and  $T(\omega) \approx 1$ . More important, the reflection

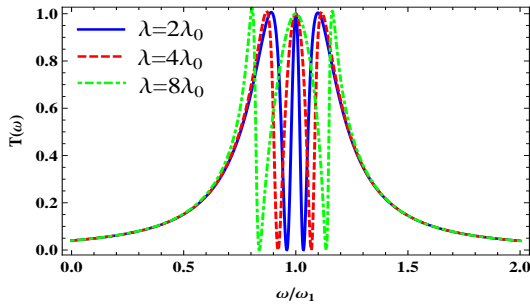


FIG. 3: (Color online) The transmission spectrum  $T(\omega)$  of the single photon as a function of normalized frequency  $\omega/\omega_1$  with different  $\lambda$  (in units of  $\lambda_0$ ,  $\lambda_0 = 10^{33}$  Hz/m<sup>2</sup>). Other parameters take the same values as in Fig. 2.

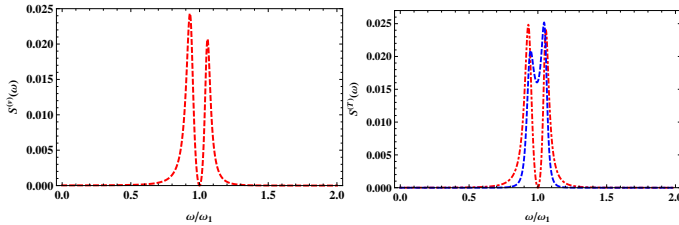


FIG. 4: (a) The vacuum noise spectrum  $S^{(v)}(\omega)$  as a function of normalized frequency  $\omega/\omega_1$ . (b) The thermal noise spectrum  $S_1^{(T)}(\omega)$  (red dotted line) and  $S_2^{(T)}(\omega)$  (blue dashed line) as a function of normalized frequency  $\omega/\omega_1$ .  $T = 20$  mK, other parameters take the same values as in Fig. 2.

and transmission spectra of a single photon exhibit other two inverted dips and two normal dips at  $\omega = \omega_1 + \omega_0$  and  $\omega = \omega_1 - \omega_0$ , here  $\omega_0$  is the small deviation from the central frequency  $\omega_1$  and it depends on the Coulomb coupling strength. We can find  $R(\omega_1 \pm \omega_0) \approx 1$  and  $T(\omega_1 \pm \omega_0) \approx 0$ . That is to say, the single photon is completely transmitted through the cavity to the right output port at frequency  $\omega = \omega_1$ , meanwhile, the single photon is completely reflected to the left two output ports with different frequencies  $\omega_1 + \omega_0$  and  $\omega_1 - \omega_0$ .

Then, we can describe the working process of the single-photon multi-output router. When we turn off the Coulomb coupling, the single photon is completely reflected through the cavity to the left output port at frequency  $\omega = \omega_1$  (*i.e.*  $R(\omega_1) \approx 1$ ,  $T(\omega) \approx 0$ ). However, when we turn on the Coulomb coupling, the single photon is completely transmitted to the right output port at frequency  $\omega = \omega_1$  (*i.e.*  $R(\omega_1) \approx 0$ ,  $T(\omega) \approx 1$ ), at the same time, three are completely reflected to the left

two outputs at different frequencies  $\omega = \omega_1 + \omega_0$  and  $\omega = \omega_1 - \omega_0$  (*i.e.*  $R(\omega_1 \pm \omega_0) \approx 1$  and  $T(\omega_1 \pm \omega_0) \approx 0$ ). Fig. 4 describes the transmission spectrum  $T(\omega)$  with different Coulomb coupling strength. From Fig. 4, we find the different output frequencies can be selected by adjusting the Coulomb coupling strength.

Next, we discuss the effects of the quantum and thermal noise on the reflection and transmission spectrum of a single-photon. From Fig. 5, the contribution of the vacuum noise maximum is about 2.5% and is thus insignificant. The thermal noise could be more critical in deteriorating the performance of the single-photon router. Clearly to beat the effects of thermal noise, the number of photons in the probe pulse has to be much bigger than the thermal noise photons. However, if we work with NMM and NMR temperatures like 20 mK, then the thermal noise term is insignificant as shown in Fig. 6.

*In conclusion.*—We have proposed an experimentally accessible tunable single-photon multi-channel routing scheme based on the hybrid optoelectromechanical system which consists of an high-quality Fabry-Perot cavity coupled to a NMR. Our proposal is essentially different from previous methods in Ref.[13–15] that we are able to directly modulate the coherent input single-photon signal into three different output ports with unit probability. More important, the two output signal frequencies can be selected by adjusting Coulomb coupling strength. We also demonstrate the vacuum and thermal noise will be insignificant for the optical performance of the single-photon router at temperature of the order of 20 mK. We hope that the quantum routing function predicted in this letter can be observed in some experiments. Our proposal may have paved a new avenue towards multi-channel router and quantum networks.

## ACKNOWLEDGMENTS

This work was supported by the Major Research Plan of the NSFC (Grant No.91121023), the NSFC (Grants No. 61378012, No. 60978009, No. 11274352 and No. 11304366), the SRFDPHEC(Grant No.20124407110009), the "973" Program (Grant Nos. 2011CBA00200, 2012CB922102 and 2013CB921804), the PCSIRT (Grant No.IRT1243). China Postdoctoral Science Foundation (Grant No. 2013M531771). Natural Science Fund for colleges and universities in Jiangsu Province (Grant No.12KJD140002).

- 
- [1] H. J. Kimble, *Nature* **453** 1023 (2008).
  - [2] M. A. Hall, J. B. Altepeter, and P. Kumar, *Phys. Rev. Lett.* **106**, 053901 (2011).
  - [3] I. C. Hoi, C. M. Wilson, G. Johansson, T. Palomaki, B. Peropadre, and P. Delsing, *Phys. Rev. Lett.* **107**, 073601

- (2011).
- [4] G. S. Agarwal and S. Huang, *Phys. Rev. A* **85**, 021801(R) (2012).
- [5] T. G. Tiecke, J. D. Thompson, N. P. de Leon, L. R. Liu, V. Vuletić, and M. D. Lukin, *Nature* **508**, 241 (2014).

- [6] W. Chen, *et al.* Science **341**, 768 (2013).
- [7] D. O' Shea, C. Junge, J. Volz, and A. Rauschenbeutel, Phys. Rev. Lett. **111**, 193601 (2013).
- [8] H. Kim, R. Bose, T. C. Shen, G. S. Solomon, and E. Waks, Nature Photon. **7**, 373 (2013).
- [9] D. E. Chang, A. S. Sorensen, E. A. Demler, and M. D. Lukin, Nature Phys. **3**, 807 (2007).
- [10] T. Aoki, A. Parkins, D. Alton, C. Regal, B. Dayan, E. Ostby, K. Vahala, and H. Kimble, Phys. Rev. Lett. **102**, 083601 (2009).
- [11] X.-S. Ma, S. Zotter, J. Kofler, T. Jennewein, and A. Zeilinger, Phys. Rev. A **83**, 043814 (2011).
- [12] X.-Y. Chang et al., arXiv:1207.7265.
- [13] K. Xia and J. Twamley, Phys. Rev. X **3**, 031013 (2013).
- [14] L. Zhou, L. P. Yang, Y. Li and C. P. Sun, Phys. Rev. Lett. **111**, 103604 (2013).
- [15] J. Lu, L. Zhou, L. M. Kuang, and F. Nori, Phys. Rev. A **89**, 013805 (2014).
- [16] W. B. Yan and H. Fan, Sci. Rep. **4**, 4820 (2014).
- [17] D. Englund, A. Majumdar, M. Bajcsy, A. Faraon, P. Petroff, and J. Vukovi, Phys. Rev. Lett. **108**, 093604 (2012).
- [18] T. Volz, A. Reinhard, M. Winger, A. Badolato, K. J. Hennessy, E. L. Hu, and A. Imamoglu, Nat. Photonics **6**, 605 (2012).
- [19] K. Nozaki, T. Tanabe, A. Shinya, S. Matsuo, T. Sato, H. Taniyama, and M. Notomi, Nat. Photonics **4**, 477 (2010).
- [20] X. Hu, P. Jiang, C. Ding, H. Yang, and Q. Gong, Nat. Photonics **2**, 185 (2008).
- [21] J. D. Thompson, B. M. Zwickl, A. M. Jayich, F. Marquardt, S. M. Girvin, and J. G. E. Harris, Nature (London) **452**, 72 (2008).
- [22] W. K. Hensinger, D. W. Utami, H. S. Goan, K. Schwab, C. Monroe, and G. J. Milburn, Phys. Rev. A **72**, 041405(R) (2005).
- [23] S. Huang and G. S. Agarwal, Phys. Rev. A **83**, 043826 (2011).
- [24] G. S. Agarwal and S. Huang, Phys. Rev. A **81**, 041803(R) (2010).
- [25] S. Weis, R. Rivière, S. Deléglise, E. Gavartin, O. Arcizet, A. Schliesser, and T. J. Kippenberg, Science **330**, 1520 (2010).

